Int. J. Heat Mass Transfer. Vol. 31, No. 2, pp. 229–239, 1988
Printed in Great Britain

0017–9310/88 $3.00 + 0.00

Nucleate boiling heat transfer and critical heat flux in narrow space between rectangular surfaces

Y. FUJITA, H. OHTA and S. UCHIDA
Department of Mechanical Engineering, Kyushu University, Hakozaki, Higashi-ku, Fukuoka, Japan

and

K. NISHIKAWA
Kurume College of Technology, Komorino, Kurume, Japan

(*Received* 2 *September* 1987)

Abstract—Pool boiling heat transfer in a confined narrow space is systematically investigated for saturated water at atmospheric pressure between heated and unheated parallel rectangular plates. Experiments are performed at heat flux from boiling inception to the critical heat flux on heating surfaces with a width of 30 mm, lengths of 30 and 120 mm, and gap sizes of 5, 2, 0.6 and 0.15 mm under three surface peripheral conditions. They are all edges open, closed side edges, and closed side and bottom edges. Space inclination is also changed from vertical to facing downwards nearly to the horizontal. On the basis of measurements and observation, boiling behavior and mechanisms in a narrow space are discussed. Measured critical heat flux under two different periphery conditions are also compared with predictions on corresponding burnout models.

1. INTRODUCTION

POOL BOILING in a confined narrow space is frequently encountered in various heat transfer equipment. In this case, heat transfer characteristics become quite different from those of conventional unconfined pool boiling. There may arise in a confined space two opposing effects either to enhance or to degrade heat transfer as compared with that for the unconfined situation. Therefore, knowledge on the effect of a confined space on heat transfer in pool boiling is of great practical importance and also of great academic interest, but it is still very limited.

Several investigations have been conducted in a confined narrow space so far. Katto and co-workers [1, 2] carried out experiments on nucleate boiling at rather high heat flux in a space bounded by two horizontal co-axial disks with the lower disk heated and they classified the boiling behavior depending on gap size into three regions as follows: unheated bubbles, depressed bubbles, and oppressed bubbles. They investigated in detail the region of depressed bubbles and pointed out the thin liquid film evaporation as a dominant heat transfer mechanism of this region. Ishibashi and Nishikawa [3] performed experiments at rather low heat flux in a vertical annuli of a heated core and unheated external shroud with both ends open. They identified the isolated bubble region and the coalesced bubble region. Compared with the unconfined situation, the enhanced heat transfer coefficient is attained in the coalesced bubble region and an empirical correlation was proposed for this region. Yao and Chang [4] studied pool boiling in a vertical annuli with a closed bottom for various gap sizes, fluids, and heat fluxes, and distinguished three boiling regimes of isolated deformed bubbles, slightly deformed bubbles, and coalesced deformed bubbles, on a boiling map where the Bond number and the boiling number are chosen as coordinates. Hung and Yao [5] measured the heat transfer coefficient and critical heat flux in a horizontal annuli with open ends, and investigated the effects of annuli length, liquid subcooling, and non-uniform gap due to eccentricity. As for the critical heat flux in a confined space, Chang and Yao [6] and Nejat [7] modified the flooding model of Wallis [8] to correlate their data in a vertical annuli with a closed bottom. Kusuda and Imura [9] clarified heat transfer in an annuli of a boiling thermosyphon with an unheated core rod.

Though considerable light has been focused on the heat transfer problem through these experimental studies in confined narrow spaces of various size and geometry under various peripheral conditions, there may still be required basic data to elucidate further the boiling behavior and heat transfer in a confined narrow space.

In the present study, systematic experiments on heat transfer characteristics in pool boiling are performed in a confined narrow space bounded by a rectangular heating surface and an opposed unheated plate. Various parameters which may affect the boiling behavior in a confined space are taken into account. They are the gap size, the peripheral condition of a space whether edges of a space are open to bulk liquid

NOMENCLATURE

A	area [m^2]	s	gap size [mm or m]
a	thermal diffusivity [$m^2 s^{-1}$]	ΔT_{sat}	wall superheat [K]
C	constant in equation (13) [—]	t	time [s]
c_f	friction coefficient [—]	v	specific volume [$m^3 kg^{-1}$]
D	characteristic dimension [m]	W	width of duct [m]
D_e	hydraulic diameter [m]	x	quality [—]
f	void fraction [—]	z	distance along duct [m].
G	superficial mass velocity [$kg m^{-2} s^{-1}$]		
g	gravitational acceleration [$m s^{-2}$]		
H	height of duct [m]	Greek symbols	
j^*	non-dimensional superficial velocity [—]	α	heat transfer coefficient [$W m^{-2} K^{-1}$]
Δh_v	latent heat of evaporation [$J kg^{-1}$]	δ	thickness of thin liquid film [m]
Nu	Nusselt number [—]	θ	inclination angle [deg]
p	pressure [Pa]	λ	thermal conductivity [$W m^{-1} K^{-1}$]
q	heat flux [$W m^{-2}$]	μ	viscosity [Pa s]
Re	modified Reynolds number defined by equation (6) [—]	ν	dynamic viscosity [$m^2 s^{-1}$]
		ρ	density [$kg m^{-3}$]
ΔR	gap size of annuli [m]	τ_w	wall shear stress [$N m^{-2}$].

or not, the longitudinal length of a space, and the inclination of a space. Heat transfer coefficient and critical heat flux are measured along with visualization of boiling behavior for saturated nucleate boiling of distilled water under atmospheric pressure at heat flux covering almost the whole nucleate boiling region. On the basis of the experimental data and observation, characteristics and mechanism of boiling in a confined space are discussed and heat transfer models and tentative prediction of heat transfer are proposed. The critical heat flux under two basically different peripheral conditions are reproduced by corresponding different burnout mechanisms.

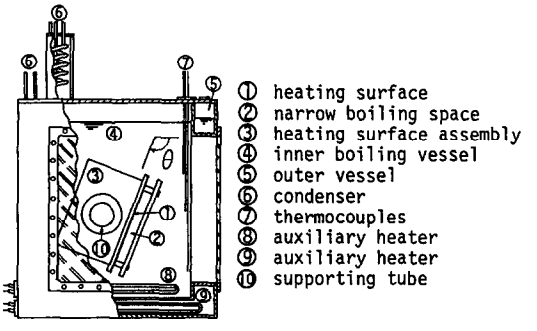

FIG. 1. Experimental apparatus.

2. EXPERIMENTAL APPARATUS AND PROCEDURE

The experimental apparatus is illustrated in Fig. 1. The heating surface assembly ③ is installed in the middle of an inner boiling vessel ④ by horizontal supporting tubes ⑩, which bring power and thermocouple leads to and from the inner vessel. These supporting tubes can be rotated around the horizontal axis to change an inclination angle of a heating surface without interrupting the boiling [10]. The heating surface consists of a rectangular copper plate, 30 mm wide and 30 mm long for Surface A, and 30 mm wide and 120 mm long for Surface B. They are surrounded by fins around their periphery so as to reduce heat loss. The fin and heating surface are cut out in a unit body to prevent preferential boiling at the edge of the heating surface. Figure 2 shows the heating surface assembly and the narrow space geometry for Surface B. The heat flux is supplied by conduction through a copper block from electric heaters ⑥ in the slits at the bottom.

Thermocouples are positioned at the center for Surface A, and at four longitudinal locations at 15, 45, 75, and 105 mm from the bottom edge for Surface B.

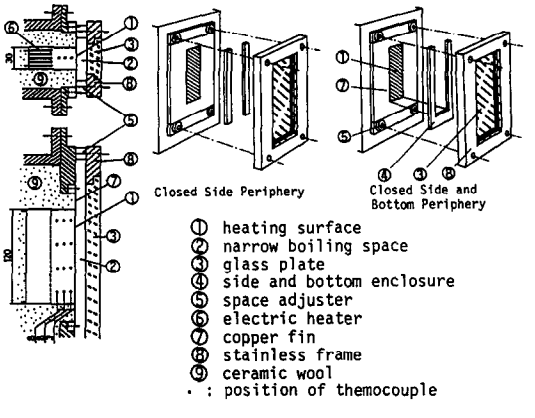

FIG. 2. Geometry of narrow space.

Small dots on the copper block in Fig. 2 indicate thermocouple positions. Their depths from the heating surface at each location are 3, 11 and 19 mm.

The narrow space is formed between the heating surface ① and the unheated glass plate ③, set face to face as shown in Fig. 2. Gap sizes of 5, 2, 0.6, and 0.15 mm are accurately set with the aid of space adjusters ⑤ of specified thickness. Three different peripheral conditions are tested, two of which are depicted in Fig. 2. The first is an open periphery where four edges of a confined space are open to bulk liquid. The second is a closed side periphery where both side edges are closed and the top and bottom edges are open. The third is a closed side and bottom periphery where only the top edge is open to bulk liquid. Thin teflon blocks are attached to close the specified edges of a confined space.

Experimental inclination angles of the heating surface measured from the horizontal plane are 90° (vertical surface), 150° and 175° (inclined surfaces facing downwards).

Heat flux is calculated by the temperature gradient measured by the thermocouples embedded in the heating block. Heating surface temperature is determined by extrapolation of the measured temperature gradient to the surface. For Surface B, average values for the four longitudinal locations are used as the representative values for the heat flux and the heating surface temperature.

Experiments are performed under the conditions of saturated nucleate boiling of distilled water at atmospheric pressure. Prior to each test run, the heating surface is finished with No. 0/5 emery paper in an attempt to keep the same surface conditions for all test runs. Heat transfer data are taken with heat flux decreasing step by step to avoid the boiling hysteresis effects. Critical heat flux is defined when the heating surface temperature starts rising gradually or suddenly in an excursion. Since heat transfer characteristics are closely related to boiling behavior, visual observation by still pictures is carried out along with heat transfer measurements.

3. EXPERIMENTAL RESULTS

3.1. *Effects of gap size and periphery condition*

Figure 3 shows the boiling curves obtained on vertical Surface B for various combinations of gap size and periphery conditions, where q is the heat flux, ΔT_{sat} the degree of superheat of the heating surface, and s the gap size. Arrows in the figure show the measured levels of critical heat flux. Typical boiling behaviors are shown in Fig. 4 for gap sizes of 5, 0.6, and 0.15 mm under the open and closed side and bottom periphery conditions. Boiling behaviors and heat transfer characteristics are summarized as follows depending on the combination of periphery condition and gap size.

3.1.1. *Open periphery.* At large gaps $s = 5$ mm, a bubble is so small compared with the gap size that

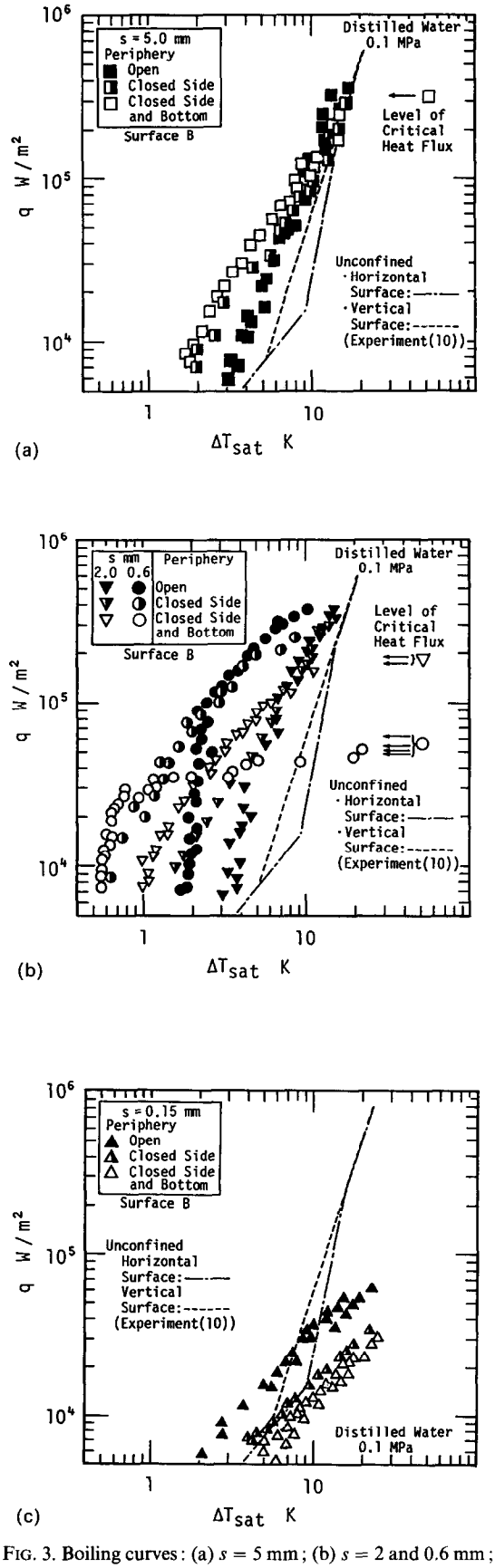

FIG. 3. Boiling curves: (a) $s = 5$ mm; (b) $s = 2$ and 0.6 mm; (c) $s = 0.15$ mm.

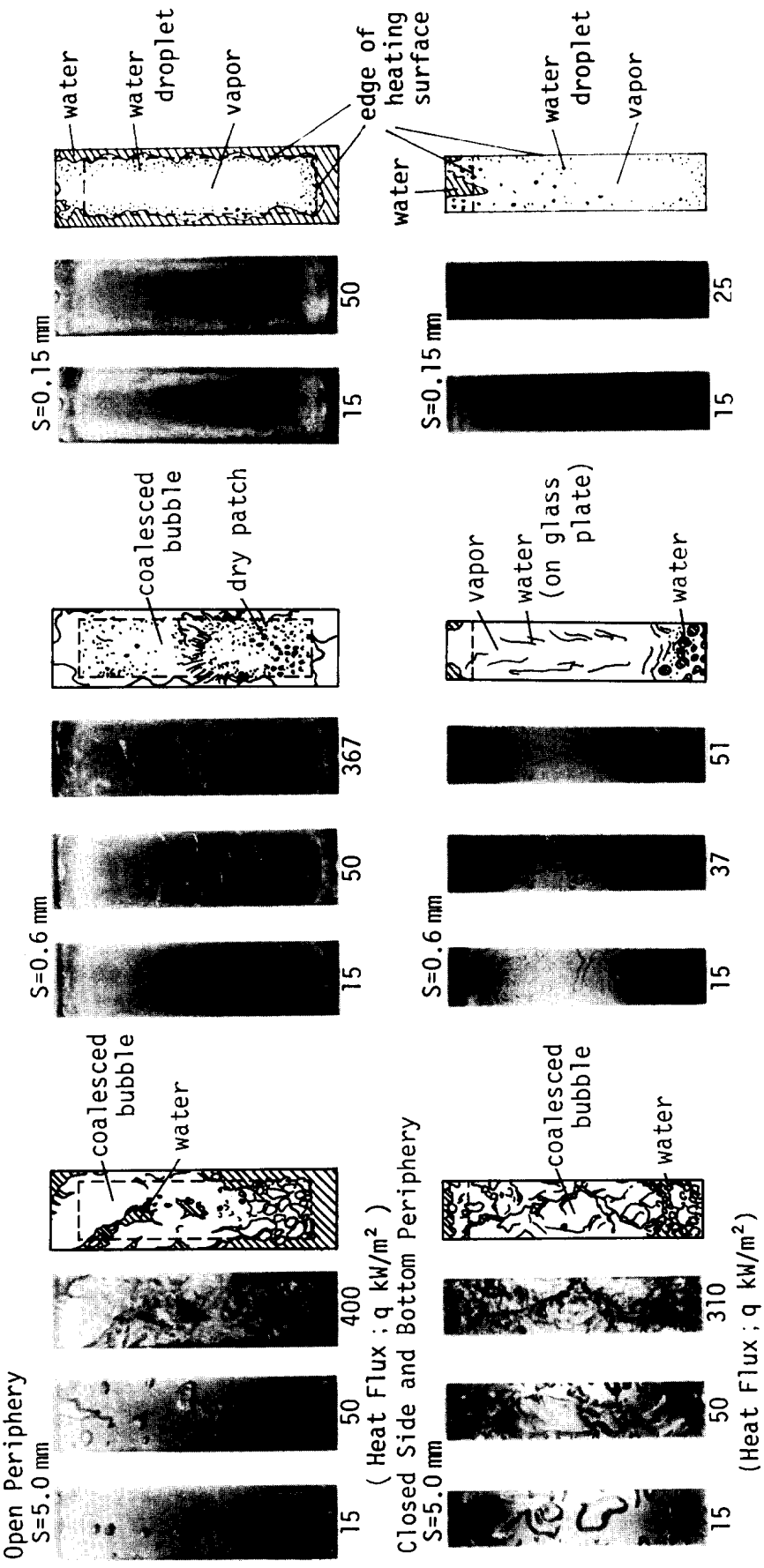

FIG. 4. Boiling behavior.

bubble behavior and the shape of boiling curves are similar in nature to those in the unconfined boiling [10]. But a higher heat transfer rate is achieved at low heat flux due to the two-phase mixture agitation in a narrow space.

At moderate gaps $s = 2$ and 0.6 mm, an isolated bubble at low heat flux is squeezed and flattened and grows rapidly to cover the width of the heating surface, enhancing heat transfer markedly. The rapid growth of a bubble and highly enhanced heat transfer are supposed to be attributable to the liquid film evaporation observed between the flattened bubbles and the heating surface. Especially at low heat flux less than about 1.5×10^5 W m^{-2}, alternative bubble generation of the periodic and the intermittent occurs depending on a delicate difference in the heating surface finish. This leads to poor reproducibility of the boiling curve. Data in the figure are those measured during the periodic bubble generation. Boiling curves during the intermittent bubble generation move to higher superheat of the heating surface. At high heat flux, bubble generation becomes more frequent and stable. Partial bubble accumulation is observed on the upper part of the heating surface, which reduces the slope of the boiling curve and therefore the enhancement rate of heat transfer.

At gap sizes $s = 0.15$ mm, most of the heating surface is steadily covered with vapor and a wavy liquid–vapor interface is observed only close to the open edges even at very low heat flux. An increase of the heat flux gives no further change in this boiling behavior. Vigorous oscillation of a standing liquid–vapor interface sometimes splashes fine droplets over the heating surface covered with vapor but they are immediately out of sight. This means that the vapor-covered portion is dried and most heat is transferred from the wetted area near the open edges. Since the wetted area is very narrow compared with the total heating surface, the heat transfer rate is less than that for unconfined boiling.

3.1.2. *Closed side periphery.* At gap sizes $s = 5$ and 2 mm, closing side edges give no marked difference in both boiling behavior and heat transfer compared with the case of open side edges. This is because liquid and vapor bubbles flow mainly in the longitudinal direction in either case.

At gap sizes $s = 0.6$ mm, retardation of rising bubbles leads, contrary to expectation, to a higher transfer rate at low heat flux than that under the open periphery condition. But this enhancement decreases at high heat flux due to vapor accumulation all over the heating surface.

At gap sizes $s = 0.15$ mm, the heating surface is completely covered with vapor and only open edges at the top and bottom are exposed to liquid. The heat transfer coefficient becomes lower than that under the open periphery condition or that for unconfined pool boiling. This implies heat transfer degradation.

3.1.3. *Closed side and bottom periphery.* At gap sizes $s = 5$ mm, liquid penetration into a boiling space is only from the open top edge. Rising bubbles are easily subject to the deformation and mixing owing to the countercurrent liquid penetration, and a coalesced bubble becomes larger than that observed for the open periphery. Heat transfer is more enhanced as a result of the countercurrent of bubble outflow and liquid inflow. At a heat flux more than about 1.5×10^5 W m^{-2}, however, generated vapor bubbles fill up the gap and hinder the steady liquid penetration into it. In this situation, liquid is supplied mainly along the unheated glass plate, synchronized with the up and down oscillations of generated vapor. Thus, the heat transfer coefficient at high heat flux becomes slightly smaller than that for the open periphery.

At gap sizes $s = 2$ and 0.6 mm, many bubbles generate and rise between the narrow space expanding their volume even at low heat flux. Rising bubbles are agitated by counter liquid penetration from the open top edge and they are divided into smaller deformed bubbles. Especially at $s = 0.6$ mm, most of the heating surface is dried already at a heat flux of about 2.5×10^4 W m^{-2}, and large liquid droplets fall down between the surface to fill the bottom space where some active nucleation sites can be found. At a heat flux of about 4×10^4 W m^{-2}, the top part of the heating surface is completely dried and liquid film falls down along the unheated glass plate. Vigorous boiling can be observed at the bottom portion. At low heat flux, in addition to heat transfer at the bubble base, agitation of the vapor–liquid mixture by the penetration of liquid from the open top edge results in a larger rate of heat transfer enhancement than that for the open periphery. At high heat flux, however, shortage of liquid on the heating surface causes a rapid fall of enhancement rate and occurrence of burnout.

At gap sizes $s = 0.15$ mm, heat transfer is more degraded than that for the closed side periphery because only the open top edge can contact with liquid.

3.2. *Effect of length of heating surface*

Figure 5 shows the boiling curves obtained on Surface A 30 mm in length and Surface B 120 mm in length at the vertical inclination, under open and closed side and bottom periphery conditions. Even under the open periphery condition, the boiling behavior for Surface A does not coincide with that observed on the lower quarter of Surface B. It rather resembles the vertically reduced behavior of Surface B. The heating surface length does not give a distinctive effect under the open periphery condition, while for the closed side and bottom periphery condition, the longer surface gives a lower heat transfer rate than the shorter surface. This is true at high heat flux for $s = 0.6$ mm and over the whole heat flux for $s = 0.15$ mm. This is due to the vapor covering the heating surface because the longer surface, higher heat flux and narrower gap cause the higher vapor velocity at the exit which hinders the liquid penetration from the open top edge.

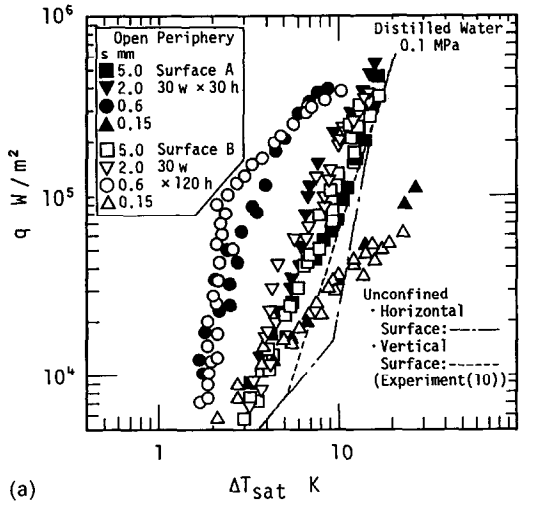

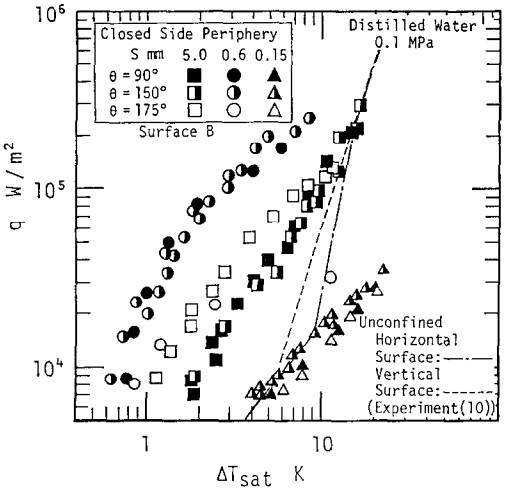

FIG. 6. Effect of surface inclination.

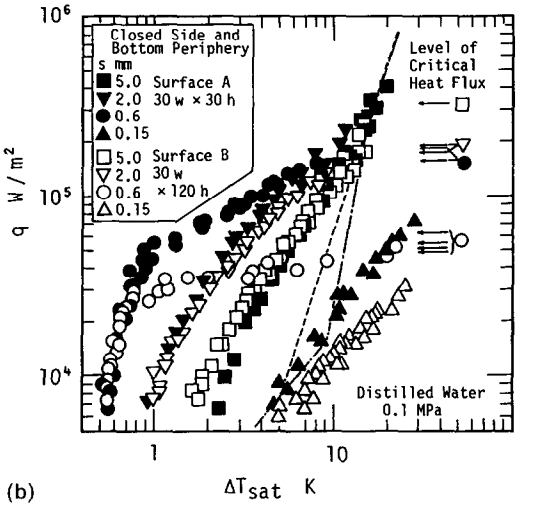

FIG. 5. Effect of length of heating surface: (a) open periphery; (b) closed side and bottom periphery.

3.3. *Effect of surface inclination*

Figure 6 shows the boiling curves on inclined surfaces under the closed side periphery condition, the inclination angles of which measured from the horizontal plane are $\theta = 90°$ (vertical surface), 150° and 175° (surfaces facing downwards). Boiling curves for $\theta = 150°$ and $s = 5$ and 0.6 mm do not deviate far from the boiling curves for the vertical surface with the same gap size. This is partly because the velocity of rising bubbles does not directly affect the heat transfer provided that the flow is stable enough to supply liquid to a heating surface.

For $\theta = 175°$, heat transfer at a gap size $s = 5$ mm is enhanced much more than that for the vertical surface. This is because flattened bubbles are pushed up to the heating surface to contact over an enlarged area and therefore the heat transfer rate increases due to thin liquid film evaporation under these bubbles. At $s = 0.6$ mm, on the contrary, inclination of the confined space results in slowly rising bubbles and vapor accumulation on the heating surface, which lead to a lower rate of heat transfer enhancement than that for the case $\theta = 90°$ or 150°.

At the narrowest gap size $s = 0.15$ mm, the heating surface is completely covered with vapor and this boiling behavior does not change with inclination angle. Consequently the boiling curves gather together for all inclination angles.

4. PREDICTION OF HEAT TRANSFER

4.1. *Prediction based on sensible and latent heat transport model for gap sizes of* 2 *and* 0.6 mm

At gap sizes of 2 and 0.6 mm, boiling curves are independent of an inclination angle of the heating surface between 90° and 150°. Especially under the open and closed side periphery conditions, heat transfer is markedly enhanced by a peculiar mechanism of the evaporation of thin liquid film formed between the heating surface and the flattened bubbles. If attention is paid to a point on the heating surface, a liquid slug and vapor bubble alternately pass over the point concerned. This situation resembles that observed on the inclined boiling surface facing downwards in an unconfined pool [10]. Thus, heat is assumed to be transferred as sensible heat and latent heat. A rising flattened bubble carries away the superheated liquid layer in front of it. The sensible heat removed in this manner is calculated as follows on the basis of one-dimensional transient heat conduction from the heating surface to the semi-infinite liquid during the liquid period t_l, defined as the time interval during which the heating surface is in contact with the liquid filling up the gap

$$q_l = \frac{2\lambda_l \Delta T_{sat}}{\sqrt{(\pi a_l t_l)}} \tag{1}$$

where λ_l and a_l are the thermal conductivity and diffusivity of liquid, respectively. Existence of the unheated

glass plate is neglected in the above equation. But this may be admissible since the thermal boundary layer scarcely reaches the glass plate even at the end of the liquid period. After the liquid period elapses, a succeeding bubble rises up and reaches the point in question. During the successive vapor period t_v, defined as the time interval during which the heating surface is covered with a rising bubble, a thin liquid film is formed and evaporated under the bubble. The latent heat removed in this manner is approximately evaluated by heat conduction through the liquid film as follows:

$$q_v = \frac{\lambda_l}{\delta}\Delta T_{sat} \tag{2}$$

where δ is the average thickness of the liquid film.

As the heating surface is alternately in contact with the liquid slug and a bubble, the time-averaged heat flux can be expressed as

$$q = \frac{q_l t_l + q_v t_v}{t_l + t_v} = (1-f)q_l + fq_v \tag{3}$$

where f is the void fraction, calculated as the time ratio of the vapor period to the total.

As the film thickness is difficult to measure in the boiling experiment, measurements were performed for a liquid film formed between the non-heating surface and an air bubble rising in a narrow gap [10]. The measured film thickness is $\delta = 34$ μm for $s = 2$ mm and $\delta = 9$ μm for $s = 0.6$ mm irrespective of the volume and frequency of an injected air bubble. These results are assumed applicable to the case of boiling bubbles. Periods t_l and t_v were measured 0.5 mm above the heating surface at vertical locations of 20 (L-position), 60 (M-position), and 100 mm (H-position) from the bottom edge, using an electric probe which detects the liquid and vapor phases. Mean values of t_l and t_v for each gap size are evaluated from statistical reduction of the measured data so as to avoid underestimating the significant contribution by the long bubble slugs. Figures 7 and 8 show the measured periods and void fraction.

Predicted heat flux from equation (3) using values on the curves through data in Fig. 7 is compared with the measured flux in Fig. 9. Good agreement is confirmed for $s = 2$ mm, while the prediction is higher for $s = 0.6$ mm and the deviation increases with heat flux. This trend of deviation implies that the heating surface is dried at some locations due to complete evaporation of the liquid film before the end of the vapor period. Visual observation supports the occurrence of the dried area.

4.2. *Prediction by Ishibashi and Nishikawa's correlation*

Ishibashi and Nishikawa [3] proposed the following empirical formulae to correlate their boiling data in the coalesced bubble region of water in a vertical annuli with both ends open:

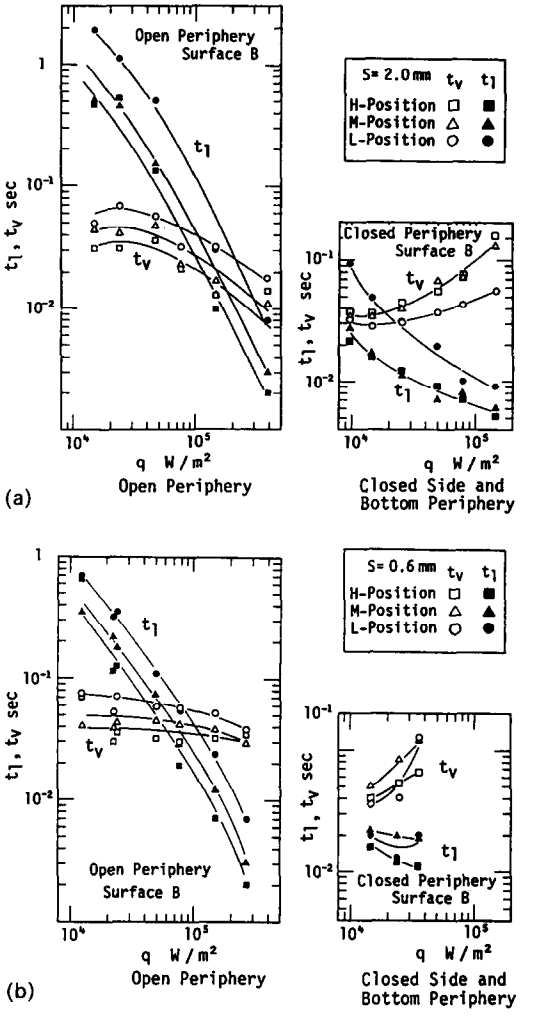

FIG. 7. Liquid and vapor periods: (a) $s = 2$ mm; (b) $s = 0.6$ mm.

$$Nu = 16.0\{Re^{1/2}\}^{2/3} \tag{4}$$

$$Nu = \frac{\alpha \Delta R}{\lambda} \tag{5}$$

$$\left.\begin{aligned} Re &= \left(\frac{q}{\Delta h_v \rho_v}\frac{\Delta R}{\nu}\right)\left(\frac{q}{q_0}\right) \\ q_0 &= 1.6\times 10^6\,\mathrm{W\,m^{-2}} \end{aligned}\right\} \tag{6}$$

where Nu is the Nusselt number, Re the modified Reynolds number, ΔR the gap size of annuli, λ the thermal conductivity of liquid, ν the dynamic viscosity of liquid, Δh_v the latent heat of evaporation, and ρ_v the density of vapor. Figure 10 shows the correlated result for the open and closed side periphery, in which the gap size s is used in place of ΔR. Data at $s = 0.15$ mm are excluded from the calculation because the boiling behavior is different from that in the coalesced bubble region. For the open periphery condition, experimental data including those at $s = 5$ mm to which the correlation should not be applied, are well correlated within an accuracy of 30 and -40%. For

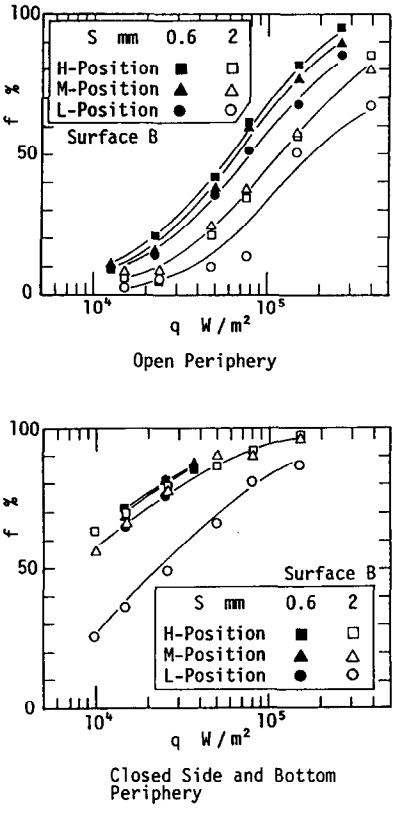

FIG. 8. Void fraction.

the closed side periphery condition, agreement is poor though this periphery condition is similar to that in a vertical annuli with both ends open for which the formulae are derived. The reason for this disagreement is uncertain at present.

4.3. *Heat transfer mechanism at gap size of* 0.15 mm

At the smallest gap size of 0.15 mm, the boiling curves run almost straight with a slope of about 45°,

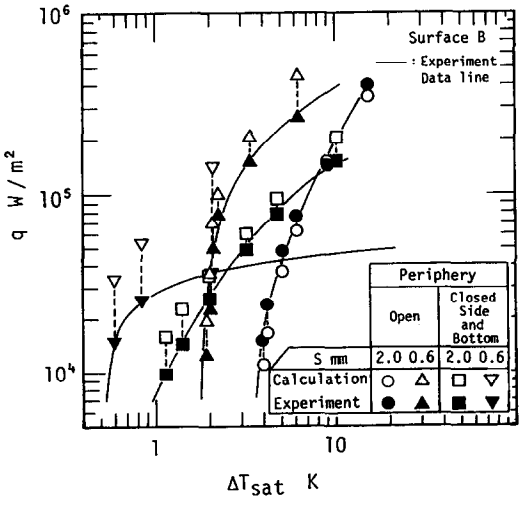

FIG. 9. Prediction by sensible and latent heat transport model.

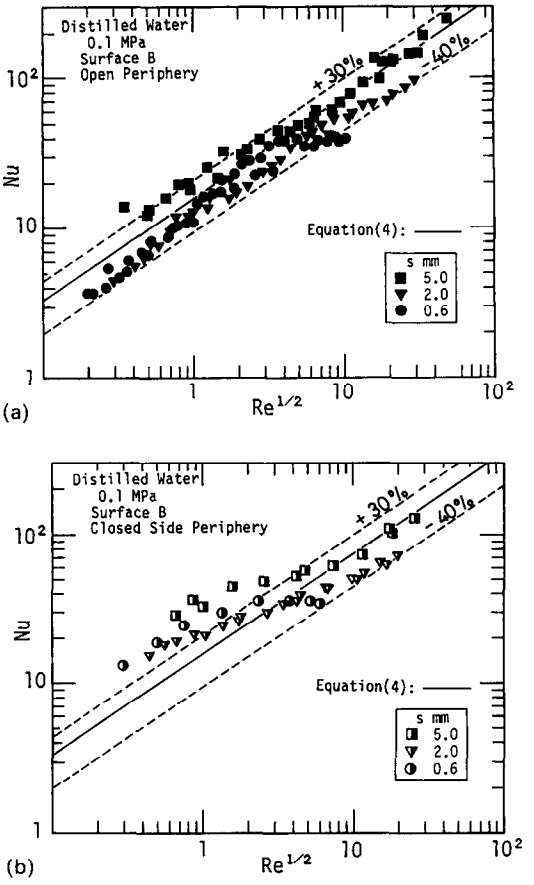

FIG. 10. Correlation of data by Ishibashi and Nishikawa's formula: (a) open periphery; (b) closed side periphery.

which means the constant heat transfer coefficient independent of heat flux or heating surface superheat. Since the wetted area is observed only in a narrow zone near the open edges, the heating surface is divided into the wetted area A_l and the remaining dried area A_v as shown in Fig. 11. Then the total heat supplied to the far end of the heating block is removed across the heating surface partly through the wetted area with heat transfer coefficient α_l and partly

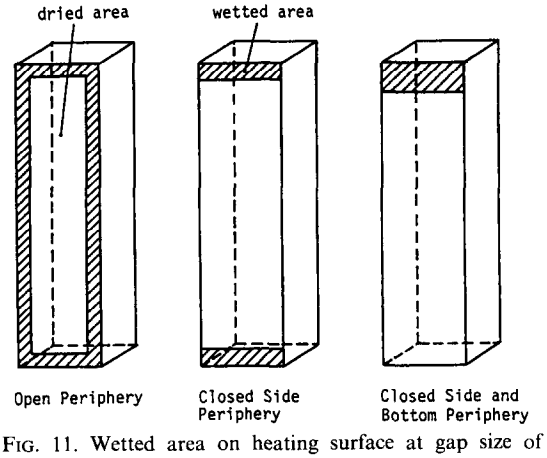

FIG. 11. Wetted area on heating surface at gap size of 0.15 mm.

through the dried area with coefficient α_v. Consequently

$$qA = \alpha_v A_v \Delta T_v + \alpha_l A_l \Delta T_l \tag{7}$$

where A is the heating surface area, and ΔT_v and ΔT_l the heating surface superheats on the dried and wetted areas, respectively. As the heating block is made of copper with a large thickness, the measured local surface temperature is quite uniform, so that $\Delta T_v = \Delta T_l = \Delta T$. There may be so great a difference between the heat transfer coefficients for both areas, that $\alpha_v \ll \alpha_l$. Thus, q is approximately proportional to ΔT provided that the heat conductance of the wetted area $\alpha_l A_l$ does not change with heat flux. The heat transfer coefficient $\alpha_l A_l / A$ becomes higher for the larger wetted area, which corresponds to the longer edge length of the open periphery.

5. PREDICTION OF CRITICAL HEAT FLUX

5.1. *Closed side periphery condition*

For the closed side periphery, critical heat flux may be predicted from the limiting condition that the homogeneous flow of the vapor and liquid mixture in a vertical duct is completely evaporated at the top exit. If the continuity and momentum equations are applied to a control volume of vertical infinitesimal length dz within the rectangular narrow duct of width W, gap size s and height H, the pressure gradient incorporates the contributions of hydrostatic, wall shear stress, and fluid acceleration terms as

$$-\left(\frac{dp}{dz}\right) = \frac{g}{v} + \frac{2(W+s)}{Ws}\tau_w + G^2\frac{dv}{dz} \tag{8}$$

where p is the static pressure, g the gravitational acceleration, v the specific volume, τ_w the wall shear stress, and G the mass velocity. The shear stress τ_w is estimated in terms of the friction coefficient as follows:

$$2(W+s)\tau_w = \frac{\pi}{2} D_e f G^2 v \tag{9}$$

where D_e is the equivalent diameter given by $2Ws/(W+s)$. The specific volume v of the vapor–liquid mixture is a function of the quality x and the specific volumes v_l and v_v for liquid and vapor. Under an assumption that heat flux is uniform, $x = 0$ at the bottom inlet, and $x = 1$ at the top exit, then $x = z/H$. Using these relations, equation (8) is easily integrated to give the pressure drop Δp between the inlet and exit, which is equated to the static liquid head gH/v_l of height H

$$\frac{gH}{v_l} = \frac{gH}{v_v}\ln\left(1+\frac{v_v}{v_l}\right) + \frac{\pi c_f G^2 H}{W+s}\left(v_l + \frac{v_v}{2}\right) + G^2 v_v \tag{10}$$

where c_f is estimated from the Blasius equation, using the mean viscosity μ_m evaluated at $x = 0.5$ from the following relation:

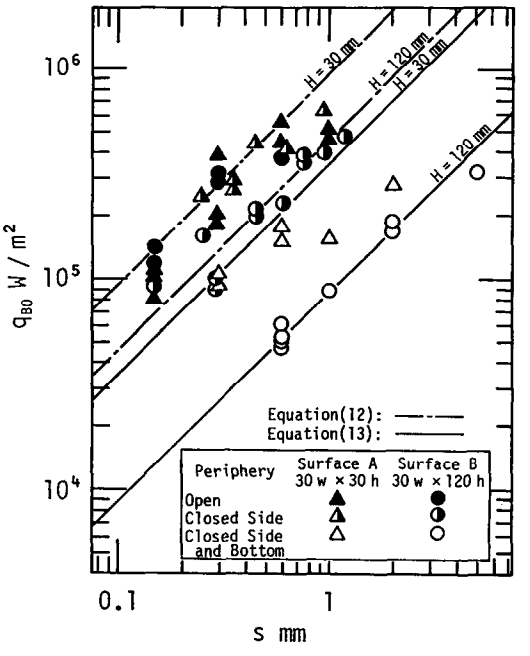

FIG. 12. Predicted critical heat flux and measured data.

$$\mu_m = \frac{1}{(1-x)/\mu_l + x/\mu_v} \tag{11}$$

where μ_l and μ_v are the viscosities of liquid and vapor, respectively. Equations (9)–(11) are solved to find the mass velocity traversing the duct. Then the critical heat flux q_{B0} becomes

$$q_{B0} = \frac{Gs\Delta h_v}{H}. \tag{12}$$

Figure 12 compares the prediction with the measurements for vertical Surface B. Even if x in equation (11) is changed from 0.1 to 0.9, the calculated value of q_{B0} changes only 2% for $s = 5$ mm and 15% for $s = 0.15$ mm. Prediction agrees well with the measurements for the closed side periphery, while it underestimates the measured results for the open periphery. This is partly due to the effect of liquid flow from the side edges.

5.2. *Closed side and bottom periphery*

When the bottom and side edges are closed, only the top edge is open to bulk liquid and the liquid supply to a confined space is done against the vapor velocity in the opposite direction. Consequently burnout may be limited by the flooding at the top edge because vapor velocity is highest at that point.

Wallis' correlation [8] for countercurrent flooding is

$$j_v^{*1/2} + j_l^{*1/2} = C \tag{13}$$

where j_v^* and j_l^* are the non-dimensional superficial velocities of vapor and liquid, respectively, at the flooding point. They are related to the superficial mass velocities G_v and G_l, which are expressed in terms of

heat flux, height of heating surface, and gap size as follows:

$$\left.\begin{aligned} j_v^* &= \frac{G_v}{\sqrt{(gD\rho_v(\rho_l-\rho_v))}} \\ j_l^* &= \frac{G_l}{\sqrt{(gD\rho_l(\rho_l-\rho_v))}} \\ G_v &= G_l = \frac{qH}{s\Delta h_v} \end{aligned}\right\} \quad (14)$$

where D is a characteristic dimension of the duct cross-section. For a rectangular channel of dimensions s by W, the larger dimension is found to be more significant. Thus the prediction of critical heat flux is done using width W in place of D. If an empirical constant C depending on the geometry at the opening is equal to 0.65, predicted heat flux agrees well with measured data as seen in Fig. 12.

6. CONCLUDING REMARKS

In nucleate boiling within a confined narrow space, the effects of gap size, the periphery condition of space, the size of the heating surface and the surface orientation on heat transfer characteristics are systematically studied through the experiments. The heat transfer coefficient increases up to a certain maximum value with decrease of the gap size at moderate heat flux, while degradation occurs for a further decrease of the gap size over the whole heat flux range. For the enhanced boiling heat transfer, a predictive method is proposed based on the consideration of heat transfer mechanisms. Burnout mechanisms are also considered for the narrow spaces of two basically different periphery conditions and the predicted critical heat fluxes are compared with the measured ones.

REFERENCES

1. Y. Katto and S. Yokoya, Experimental study of nucleate pool boiling in case of making interference-plate approach to the heating surface, *Proceedings of 3rd Int. Heat Transfer Conference*, Vol. 3, pp. 219–227 (1966).
2. Y. Katto, S. Yokoya and K. Teraoka, Nucleate and transition boiling in a narrow space between two horizontal, parallel-disk surfaces, *Bull. J.S.M.E.* **20,** 638–643 (1977).
3. E. Ishibashi and K. Nishikawa, Saturated boiling heat transfer in narrow spaces, *Int. J. Heat Mass Transfer* **12,** 863–894 (1969).
4. S. C. Yao and Y. Chang, Pool boiling heat transfer in a confined space, *Int. J. Heat Mass Transfer* **26,** 841–848 (1983).
5. Y. H. Hung and S. C. Yao, Pool boiling heat transfer in narrow horizontal annular crevices, *J. Heat Transfer* **107,** 656–662 (1985).
6. Y. Chang and S. C. Yao, Critical heat flux of narrow vertical annuli with closed bottoms, *J. Heat Transfer* **105,** 192–195 (1983).
7. Z. Nejat, Maximum heat flux for countercurrent two phase flow in a closed end vertical tube, *Proceedings of 6th Int. Heat Transfer Conference*, Vol. 1, pp. 441–444 (1978).
8. G. B. Wallis, *One-dimensional Two-phase Flow*, p. 336. McGraw-Hill, New York (1969).
9. H. Kusuda and H. Imura, Boiling heat transfer in an open thermosyphon, *Bull. J.S.M.E.* **16,** 1723–1740 (1973).
10. K. Nishikawa, Y. Fujita, S. Uchida and H. Ohta, Effect of surface configuration on nucleate boiling heat transfer, *Int. J. Heat Mass Transfer* **27,** 1559–1571 (1984).

TRANSFERT THERMIQUE PAR EBULLITION NUCLEEE ET FLUX CRITIQUE DANS UN ESPACE ETROIT ENTRE DES SURFACES RECTANGULAIRES

Résumé—L'ebullition en réservoir dans un espace très étroit est étudiée systématiquement, pour de l'eau saturée à pression atmosphérique, entre deux plaques rectangulaires parallèles. Des expériences sont faites pour des flux depuis le début de l'ébullition jusqu'à la criticité sur des surfaces chaudes ayant une largeur de 30 mm, des longueurs de 30 et 120 mm et des écartements de 5, 2, 0,6 et 0,15 mm, et soumises à trois conditions périphériques de surface. L'inclinaison de la cellule est chargée entre la verticalité et l'horizontalité. Les mécanismes de l'ébullition dans un espace étroit sont discutés à partir des mesures et de l'observation. Le flux critique de chaleur dans les différentes conditions périphériques est comparé avec les prévisions des modèles correspondants.

DER WÄRMEÜBERGANG BEIM BLASENSIEDEN UND DIE KRITISCHE WÄRMESTROMDICHTE IN ENGEN SPALTEN ZWISCHEN RECHTECKIGEN PARALLELEN PLATTEN

Zusammenfassung—Der Wärmeübergang beim Behältersieden in einem engen geschlossenen Spalt zwischen beheizten und unbeheizten parallelen rechteckigen Platten wird für gesättigtes Wasser bei Atmosphärendruck systematisch untersucht. Die Versuche werden vom Siedebeginn bis zur kritischen Wärmestromdichte an den Heizflächen, die eine Breite von 30 mm und eine Länge von 30 und 120 mm haben, durchgeführt. Es werden Spaltbreiten von 5, 2, 0,6 und 0,15 mm unter drei äußeren Bedingungen untersucht. Die äußeren Bedingungen sind: alle Kanten offen, geschlossene Seitenkanten und geschlossene Seiten- und Unterkanten. Der Neigungswinkel der Spalte wird ebenfalls von vertikal bis nahezu horizontal nach unten gerichtet variiert. Auf der Grundlage der Messungen und der Beobachtungen werden das Siedeverhalten und die Siedemechanismen eines engen Spaltes diskutiert. Die bei zwei unterschiedlichen äußeren Bedingungen gemessenen kritischen Wärmestromdichten werden mit Berechnungen nach entsprechenden Burnout-Modellen verglichen.

ТЕПЛООБМЕН ПРИ ПУЗЫРЬКОВОМ КИПЕНИИ И КРИТИЧЕСКИЙ ТЕПЛОВОЙ ПОТОК В УЗКОМ ПРОСТРАНСТВЕ МЕЖДУ ПРЯМОУГОЛЬНЫМИ ПОВЕРХНОСТЯМИ

Аннотация—Теплообмен при кипении в большом объеме в ограниченном узком пространстве между нагреваемой и ненагреваемой параллельными прямоугольными пластинами изучается для насыщенной воды при атмосферном давлении. Эксперименты проводились при тепловом потоке—от начала кипения до критического—на нагреваемых поверхностях шириной 30 мм и длиной от 30 до 120 мм, величина зазора равнялась 5; 2; 0,6 и 0,15 мм при трех различных условиях на поверхностях: со всеми торцами открытыми, с закрытыми боковыми торцами и закрытыми боковыми и нижним торцами. Изменялся угол наклона пространства от вертикали почти до горизонтали. На основе измерений и наблюдений обсуждаются механизмы кипения, происходящие в узком пространстве. Измеренный критический тепловой поток при двух различных условиях на границах также сравнивается с расчетами соответствующих моделей кризиса кипения.